Cortical dynamics of perception and decision in sensory tasks: an MEG study

Lucia M. Vaina[1,2], Kunjan D. Rana[1], Matti Hamalainen[2]

[1]Brain and Vision Research Laboratory, Department of Biomedical Engineering, Boston University, Boston, MA, USA
[2]Massachusetts General Hospital, Harvard Medical School, Department of Neurology&Radiology, Boston, MA, USA
vaina@bu.edu, kdrana@bu.edu, msh@nmr.mgh,harvard.edu

Introduction

Perception and perceptual decisions arise from the spatiotemporal orchestration of activity distributed across brain networks. Functional MRI (fMRI) studies have shown that discrete networks mediate the sensory processing and the representation of visual search task[1]. However, fMRI does not have the temporal precision required for revealing the dynamic cortical networks that integrate sensory information and coordinate the decision making process during perceptual tasks. Here we used anatomically constrained (by MRI) and magnetoencephalography (MEG) to compute the temporal signature and the oscillatory synchrony that modulates cortical interactions in two search tasks. In one, VS, visual, moving observers search for a moving object (target), and in the other, VAS, an auditory cue congruent with the target facilitates performance on the task.

To understand where, when, and how cortical areas connect to each other during these tasks, in both time- and frequency- domains (α, β, and γ bands), we compared the direction and dynamics of the cortical networks using Granger causality in the time domain (DGC) and PLV in the frequency domain in 8 healthy observers.

Stimuli and Task

The stimuli (adapted from 1,2) consisted of: one second fade-in of nine textured spheres (1.5 degrees in diameter); one second static frame displaying the 9 static spheres; one second where 8 of the spheres, randomly selected, portray simulated forward motion of the observer, and the other sphere (target) moves independently with its own speed and looming motion (forward or backward). In the following 3 seconds the spheres are again shown static but numeric labels (1-4) are shown on four spheres, one of which is the target. In a 4AFC subjects indicated via a button press which was the target sphere. Percent correct and reaction times were collected. Two conditions of the experiment were run: Visual-only (V-O), and Visual-Auditory (V-A). In the latter, a suprathreshold auditory pure tone is colocalized and in % of trials moves in depth congruent with the target, while in the other % of trials is static.

Figure 1

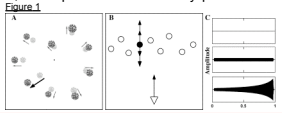

ROI Selection

ROIs (shown below) were chosen based on fMRI activation of the same task for the visual-only condition, and on MEG activation in both conditions, guided by the Freesurfer anatomical parcellation.

Figure 2

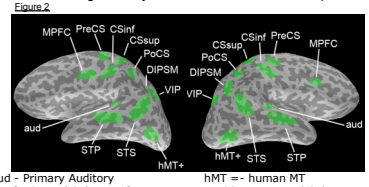

Aud - Primary Auditory
Csinf - Central Sulcus, Inferior
Cssup - Central Sulcus, Superior
DISPM = Dorsal Intraparietal Sulcus
ITS - Inferior Temporal Sulcus
MPFC - Middle Prefrontal Cortex
hMT =- human MT
PreCS - Precentral Sulcus
PoCS - Postcentral Sulcus
STP - Superior Temporal Polysensory Area
STS - Superior Temporal Sulcus
VIP - Visual Intraparietal

MEG Acquisition

MEG datasets were acquired in a magnetically shielded room using a whole head 306-channel MEG (VectorView, Elekta-Neuromag, Helsinki, Finland) The MEG signals were band-pass filtered to the frequency range 0.5 – 200 Hz and digitized at 600 samples/s. There are 102 measurement locations each equipped with three sensors, one magnetometer and two planar gradiometers. Vertical and horizontal electrooculogram (EOG) measurements were also recorded to monitor eye-movement artifacts. For stimulus presentation we employed a DLP projector and a back-projection screen, plastic tubes connected to frequency-compensated loudspeakers outside the magnetically shielded room (ADU1c, Unides Design, Helsinki). Responses were recorded with a fiber-optic response pad.

Time Windows

The stimulus is split into four time windows: T1: sensory (150 - 450 ms), T2: representation (450 - 1150 ms), T3: decision 1 (1150 - 1500 ms), T4: decision 2(1500 ms - 2000 ms).

Behavioral Results

Figure 2

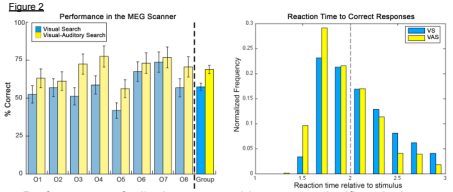

- Performance of all observers subjects was significantly better when auditory cues were available (proportions test[7] VS vs VAS: p= 2.561x10-8) .
- Given the small number of trials obtained during the imaging sessions, RT analysis should be considered more descriptive than quantitative. However, they are important here to show that in all subjects most of the responses occurred within the first 2 seconds of the stimulus, in particular starting at around 1.5 seconds from stimulus onset. Thus subjects made their decision in both VS and VAS tasks within the T4 time window.

Onset Timing

We consider an onset to occur in an ROI if its average time course within a time window exceeds 3 SD of the noise level computed from the 500 ms prestim baseline and lasts least 20 ms above this level (Raij et. al., 2010). We utilize the bootstrap method (250 bootstrap samples across epochs) and apply an approximate permutation test (using 1000 permutations) to compare timings across test conditions (VS/VAS). Group statistics are computed through Fisher's method. False Discovery Rate (FDR) control is applied to the resulting p-values with an FDR of 0.001. The table below shows which condition has faster onsets in each time window.

overall, the areas during the Visual Search (VS) condition are activated faster than in Visual Auditory Search (VAS).

	T1	T2	T3	T4
CSinf				VS
CSsup		VS		
DIPSM		VS		VAS
ITS	VS			VS
MPFC	VS	VS		VAS
hMT	VS	VS		VS
PoCS		VAS		VS
PreCS		VS		VS
STS	VS	VS	VS	VS
STP		VS	VS	
VIP	VS			VS

	T1	T2	T3	T4
CSinf			VS	VS
CSsup			VS	VS
DIPSM	VS		VS	
ITS	VS	VS	VAS	
MPFC			VAS	VS
hMT	VS			VS
PoCS		VS	VS	VS
PreCS			VS	VS
STS	VS			VAS
STP	VS			VAS
VIP		VS	VS	VS

Time-domain Cortical Connectivity

We compute temporal cortical connectivity through Granger Causality methods, which allow for the study of causal connections between cortical areas. We employ both time and frequency domain dynamic Granger-Geweke causality to investigate the transient connections between our cortical areas. Granger causality is calculated over a sliding window allowing for the study of transiently-active Granger causal connections over time.

We take 30 random sets of 50% of the total trials and we compute averaged ROI time courses for each set. Time series are temporally de-meaned and detrended. We compute the optimal sliding window size and AR order through the SURE criterion. For time-domain Granger causality, each time point's statistic is calculated using the residuals of prediction with the optimal AR model over the window given only its own time series, y, over the residuals when also provided the additional time series x:

$$G_{x\to y} = \ln\left(\sum_{i=1}^{n}\varepsilon_y^2(t)\Big/\sum_{i=1}^{n}\varepsilon_{y,x}^2(t)\right)$$

For frequency domain Granger causality, each time point's statistic is calculated using:

$$G_{x\to y}(f) = -\ln\left(1-\frac{(\Sigma_{xx}-\Sigma_{xy}^2/\Sigma_{yy})\,|H_{xx}(f)|^2}{S_{yy}(f)}\right)$$

We compute the statistic for every time point in the time domain and, due to computation time constraints, every 40 ms.

In time-domain dynamic Granger causality, a t-statistic is obtained for each datapoint by testing the set of granger scores in a part of the prestimulus (-500ms to -200ms) to the set of granger scores at a certain time point. The same is done in the frequency domain, but this is computed separately for each sampled frequency (1 Hz sampling, 5-120 Hz).

Due to the large density of connections produced by the time domain, we use the data from the frequency domain representation to compute the temporal snapshots below. For each time point, the statistic is averaged over the highest 15 scores across all frequencies for each directed connection between two ROIs. The resulting value is thresholded at a -log10 P-value of 3.5, so that any edge that is less significant is thrown out.

Dynamic Granger Causality Network Snapspots: Results

In Fig 3, we show snapshots of dynamic Granger to illustrate the dynamics of the time-varying network.

· In the early time windows (T1,T2) the main cortical interactions occur between areas involved in the sensory processing and computation of the representation, both modulated by attention and working memory. In T4, decision making stage, there is significant interaction between areas encoding the representation and the frontal areas involved in working memory (for maintenance of the representation) and decision making.

Figure 3

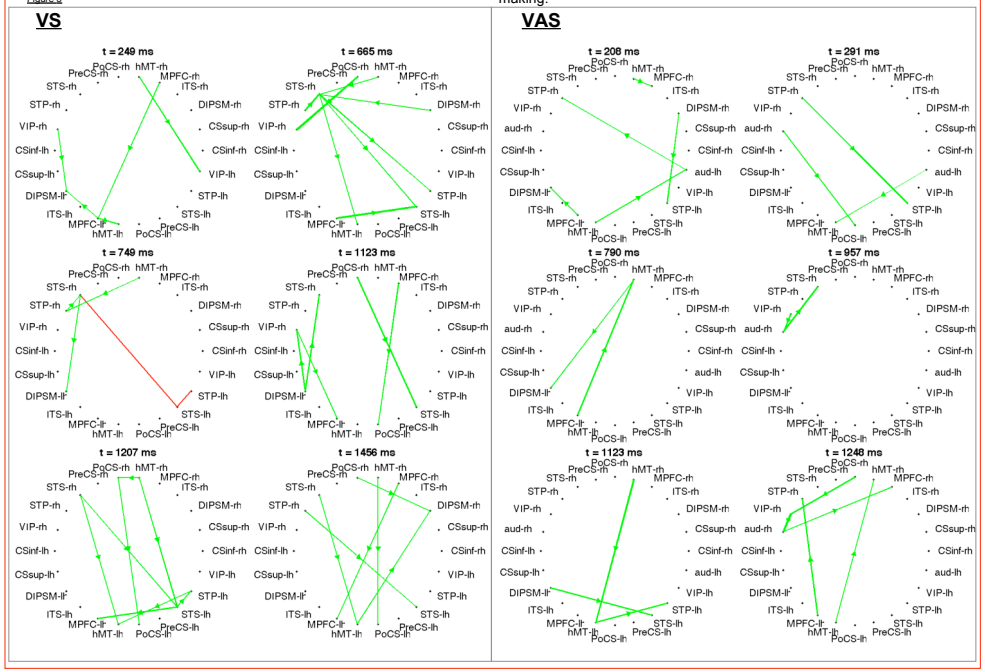

· In the VAS task, there is an early and transient connection of the **Aud** area with visually responsive areas. These connections no longer exist later on, when the mutimodal area (**STP**) have integrating visual-auditory information. The **Aud** area is again connected late (in T3&T4) in a network possibly involved in checking the detection of the target object.

· In T3 the unimodal VS network is significantly more connected than the VAS network, suggesting that the computation of the representation might be more difficult (without the benefit of additional cues).

Time-Domain and Frequency-Domain Dynamic Granger Causality: Results

Below we show sample frequency dynamic granger (top plots) and time-domain dynamic granger (bottom) for VS and VAS.

Figure 4

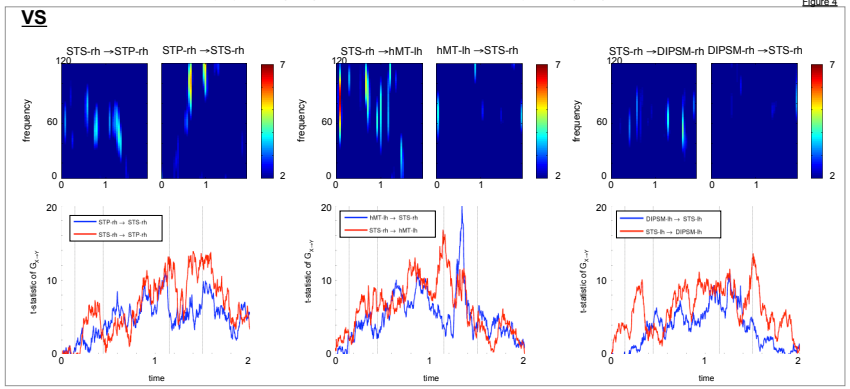

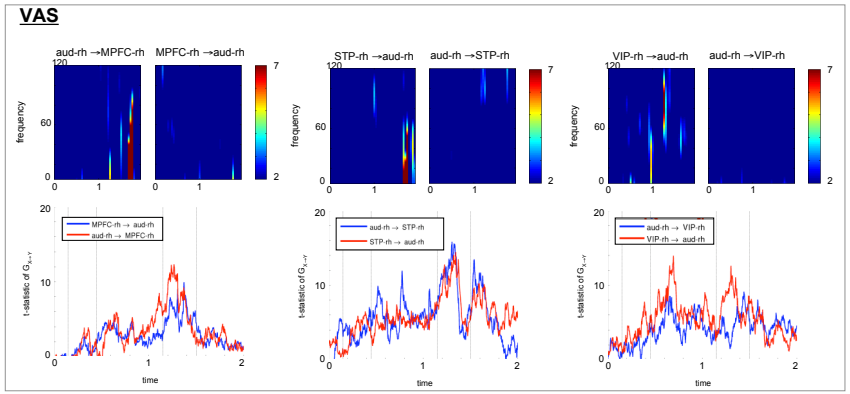

· In VS task, the network seeded on **STS**, this area is significantly sustained and reciprocally connected with **MT**, **STP**, and **DIPSM** suggesting their continuous interaction during stimulus representation, decision and selection of response. The network extends to both hemispheres involving the same cortical areas (L-hem not shown).

· In VAS there is an early but transient connection of the **Aud** to **STP**, which returns as reciprocal connection in T3. This pattern would suggest that once **Aud** has provided information to STP this area will be involved in building the multimodal representaton of the target. The **Aud** interaction returns at the level of consolidation the representation and decision making (T3&T4).

· **Aud** is also strongly connected with **MPFC**, in T3, using working memory in the target selection in the 4AFC choice task. In both, the VS and VAS tasks, (results not shown) there is strong connectivity in T3 with **DIPSM**, **STS** and **STP**, all significantly involved in the tasks representation network.

Frequency-domain Cortical Connectivity

Due to the large-banded nature of Frequency-Domain Granger-Geweke causality, we investigate the frequency domain in more detail using other methods (TFR and PLV). We are interested in the α band (5-15 Hz), the β band (15-30 Hz), and the γ band (30-50 Hz).

We study the frequency domain by observing the amplitude of activity at different frequencies through the time-frequency representation (TFR) (Fig 5) and the phase coherence between ROIs through phase locking (Fig 6-8).

Time Frequency Representation

In order to assess the levels of activity at various frequencies, the complex Morlet wavelet filter is applied to the data. Each sensor measurement is passed through the complex Morlet wavelet transform from 5 Hz to 120 Hz at 1/3 Hz intervals. Then, the wavelet transformed coefficients are mapped back onto the cortex by applying the MNE inverse solution the surface normal signal at each vertex. The magnitudes of the complex coefficients are used to infer activity at each frequency and time point. The magnitudes between 0 and 2 seconds are normalized by the average magnitude in the baseline (-0.5 to 0 seconds), producing scores equivalent to those in the dSPM

Figure 5

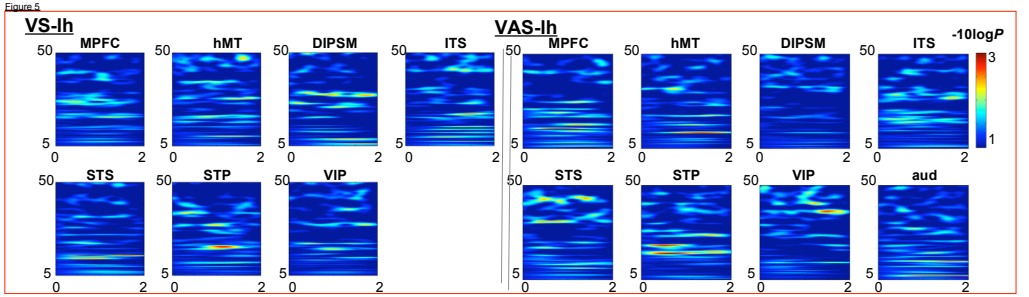

Frequency Granger in Windows

Frequency Granger causality is computed over the entire windows for T1-T4. The statistic is computed using the same frequency granger method discussed in the previous section across each frequency band (sampled at every 1 Hz in each band). The resulting statistics are summed over the frequency band of interest. Through the permutation method, multiple samples of the distribution of the null granger score are found by permuting the time courses. We test significance by comparing the true statistic to the null distribution, with a significance threshold of 0.05. To combine across subjects, we use Fisher's method. To correct for multiple comparisons, we apply the False Discovery Rate (FDR) method.

Figure 9

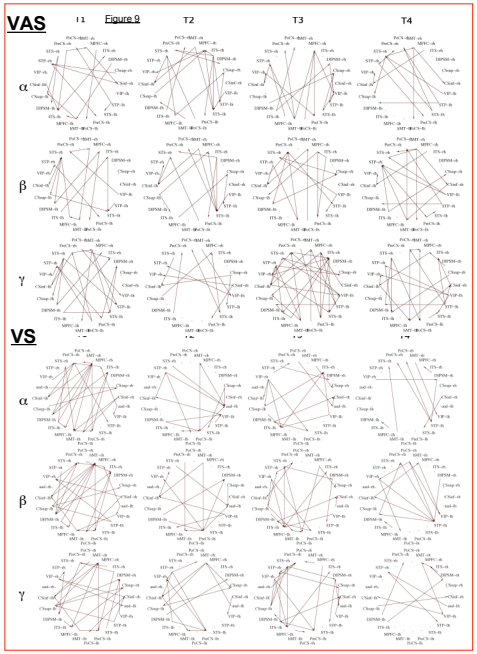

· In the VS task the frequency directionally connected networks show a progressive increase in connectivity from T1 to T3, and across frequency bands from low (alpha) to high (gamma)

· In the networks representing phase and time related connectivity during the VAS task, **MT** represents a source of outgoing and incoming connections in T1 and in T2-T4 the networks remain sparse.

Phase Locking

Dynamic frequency-band correlations are discovered between each pair of ROIs through phase locking. The trial-by-trial ROI time courses are decomposed into complex time-frequency coefficients through the Morlet wavelet transform. Phase differences are computed between two ROIs by finding the difference between the phase angles of the Morlet wavelet coefficients at corresponding trials, times, and frequencies. For each pair of ROIs at each frequency, the phase difference across trials in the prestimulus from -500 to -200 ms is compared against the phase difference at each time point across trials during the two-second stimulus interval using the Uniform-Scores Test. The test statistic is fit to a χ^2 distribution (df=2) to obtain p-values, using Fisher's method[8] to combine controls.

Figure 6

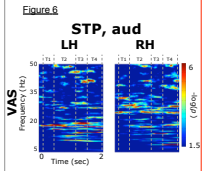

Figure 7

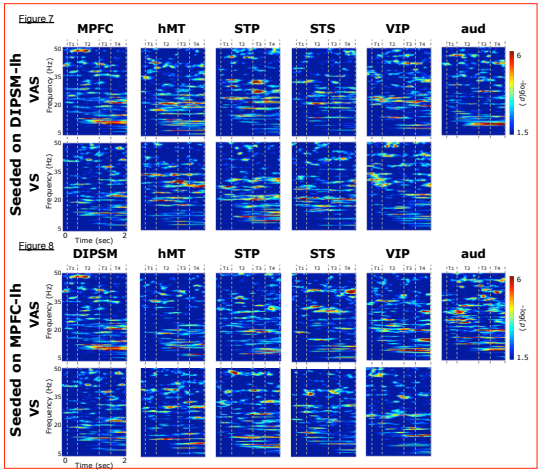

Figure 8

· Fig 6 shows significant correlation in T1&T2 between **STP** and **AUD** in the VAS task; there is more significant and sustained correlation in the gamma-band in the RH, suggesting an involvement in the representation of the multimodal target object in **STP**. Phase Locking in the L hemisphere, is earlier in the beta band. In T3&T4 periods there is more significant gamma band correlation in the L hemisphere, where presumably the task is represented.

· Fig 8 (MPFC) shows a higher coherence at all frequency bands between **MPFC** and **MT** in the VS task than in VAS. **Aud** and **DIPSM** regions are coherent with **MPFC**, first in the beta band and later in the gamma band.

· Strong and sustained gamma and beta band coherence are seen between **DIPSM** and other cortical areas involved in both VS and VAS tasks, suggesting the importance of his area in the representational networks.

References

1. Calabro, F. J., & Vaina, L. M. (in press). Detection of object motion during self-motion: psychophysics and neuronal substrate. (2011) Journal of Vision.2. Lin, F.H., et al., *Spectral spatiotemporal imaging of cortical oscillations and interactions in the human brain*. Neuroimage, 2004. **23**(2): p. 582-95. 3. Vaina, L., et al., *Long-Range Coupling of Prefrontal Cortex and Visual (MT) or Polysensory (STP) Cortical Areas in Motion Perception*. BIOMAG2010, IFBME Proceedings Series, Springer Verlag IFBME., 201 0.4.Calabro, F.J., S. Soto-Faraco, and L.M. Vaina, *Acoustic facilitation of object movement detection during self-motion*. Proceedings of the Royal Society of London B., 2011. **In press**.5.Alhvenines, J., et al., *Attention-driven auditory cortex short-term pl asticity helps segregate relevant sounds from noise*. Proc Natl Acad Sci U S A, 2011. **108**(10): p. 4182-7.6.Raij, T., et al., *Onset timing of cross-sensory activations and multisensory interactions in auditory and visual sensory cortices*. Eur J Neurosci. **31** (10): p. 1772-82.7.Newcombe R.G. *Interval Estimation for the Difference Between Independent Proportions: Comparison of Eleven Methods*. Statistics in Medicine,1998. **17**, 873–890.8.Stouffer, S.A. et al., *The American Soldier, Vol.1: Adjustment during Army Life*. Princeton University Press, Princeton, 1949.9.Z. Fisher, R.A. *Statistical Methods for Research Workers*. Oliver and Boyd (Edinburgh), 1925. ISBN 0050021702.

Acknowledgements: *NIH-R01 NS064100 to LMV and NIH-P41 RR14075 to MSH*